

Thermal Conductivity Augmentation of Composite Polymer Materials with Artificially Controlled Filler Shapes

Xiao-Jian Wang, Li-Zhi Zhang, Li-Xia Pei

Key Laboratory of Enhanced Heat Transfer and Energy Conservation of Education Ministry, School of Chemistry and Chemical Engineering, South China University of Technology, Guangzhou 510640, China

Correspondence to: L. Z. Zhang (E-mail: Lzzhang@scut.edu.cn)

ABSTRACT: Plastics or polymers of high thermal conductivity are highly desired in various industries. Adding fillers of high thermal conductivity to the base materials is a solution to make composite plastics of high thermal conductivity. Previous researches were focused on increasing the thermal conductivity of the composite materials by increasing the filler content and the thermal conductivity of the fillers. Relatively little attention was paid to the optimization of filler shapes. In this study, the effects of the filler shapes on the thermal conductivity of the composite materials are investigated, where the filler shapes are artificially designed. Heat conduction between the base materials and the artificially designed fillers is modeled. It is found that the filler shapes have great impacts on the effective thermal conductivity of the composite materials. Of the various shapes, the double Y shaped fillers are found to be the best choice for composite materials in which the fillers are distributed randomly. In future industrial applications, new filler shapes, such as double Y, Y, quad Y shaped, I and T shapes should be specially produced to replace the traditional fillers shapes: particles, fibers or slices. At last, composite materials made of paraffin wax and steel fillers of ten shapes are fabricated to simulate and validate the results. © 2013 Wiley Periodicals, Inc. *J. Appl. Polym. Sci.* **2014**, *131*, 39550.

KEYWORDS: thermal properties; theory and modeling; nanotubes; graphene and fullerenes

Received 30 March 2013; accepted 15 May 2013

DOI: 10.1002/app.39550

INTRODUCTION

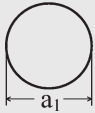
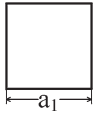
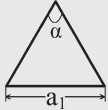
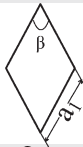
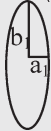
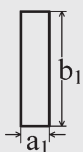
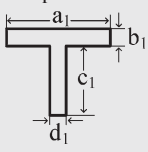
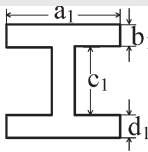
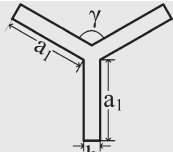
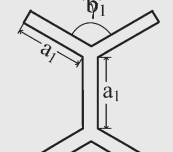
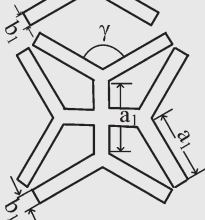
Heat exchangers are the key equipments in various industries like air-conditioning, power plants, petroleum production, chemical processes, and so on.¹ Conventional heat exchangers are mainly made of monolithic metals and metal alloys. Metal are applied extensively. Regretfully, metal corrosion in acid environment is a serious problem for traditional metal heat exchangers. It is estimated that 90% of heat exchanger damage is caused by metal corrosion. The direct economic losses from this amounted to nearly \$40 billion every year.² To solve this problem, polymers instead of metals have been used as the materials to make heat exchangers.^{3–6} However, the thermal conductivity of polymers is very low, usually in the order of $0.2 \text{ W m}^{-1}\text{K}^{-1}$.⁷ In comparison, the thermal conductivity of stainless steel is around $20 \text{ W m}^{-1}\text{K}^{-1}$.⁸ The low thermal conductivity of polymers makes the overall heat transfer coefficients of plastic heat exchangers very low. The consequence is that a larger heat transfer area is required to offset this shortcoming, which makes the plastic (polymer) heat exchanger very bulky.

To increase the thermal conductivity of polymers, adding fillers of high conductivity to the base materials has been practiced as

an efficient method to make new materials for heat exchangers.⁹ Investigated fillers include graphite, carbon black, carbon fibers, ceramic or metal particles, carbon nanotubes.^{10–12} In this way, the thermal conductivity of the plastics is increased while their virtue to resist corrosion can be largely kept.¹³

It is generally believed that filler content and its thermal conductivity are the two dominant factors influencing the overall effective thermal conductivity of polymer composites. Previous work and various correlations were mainly focused on these two respects.^{14–24} Many efforts were spent in increasing the thermal conductivity of the composite materials by either increasing the filler content²⁵ or increasing the conductivity of fillers.²⁶ These studies only considered simple filler shapes like spheres and fibers.^{27–32} Relatively little attention has been paid to the roles of artificially designed complex filler shapes. It is believed that the effective thermal conductivity of the composite materials is not a simple mixing between the fillers and base materials. Rather, artificially controlled complex filler shapes would have great impacts on the final thermal conductivity of the filled composite materials. The topic will be investigated in this research. This is the novelty of this study.

Table I. The Shapes of Fillers and Their Parameters

| Filler Name | Shapes | Shape parameters | Edge length (mm) |
|------------------------|---|---|--|
| Spherical |  | | $a_1=1.13$ |
| Square |  | | $a_1=1.00$ |
| Equilateral triangular |  | $\alpha = 60^\circ$ | $a_1=1.52$ |
| Rhombic |  | $\beta = 60^\circ$ | $a_1=1.10$ |
| Elliptical |  | $\frac{a_1}{b_1} = \frac{1}{3}$ | $a_1=0.33$ $b_1=0.99$ |
| Rectangular |  | $\frac{a_1}{b_1} = \frac{1}{4}$ | $a_1=0.50$ $b_1=2.00$ |
| T shaped |  | $a_1 = 5b_1 = \frac{5}{4}c_1 = 5d_1$ | $a_1=1.65$ $b_1=d_1=0.33$ $c_1=1.32$ |
| I shaped |  | $a_1 = 5b_1 = \frac{5}{3}c_1 = 5d_1$ | $a_1=1.35$ $b_1=d_1=0.27$ $c_1=0.81$ |
| Y shaped |  | $\frac{a_1}{b_1} = 5$ $\gamma = 120^\circ$ | $a_1=1.27$ $b_1=0.26$ |
| Double Y shaped |  | $\frac{a_1}{b_1} = 5$ $\gamma = 120^\circ$ | $a_1=1.00$ $b_1=0.20$ |
| Quad Y shaped |  | $\frac{a_1}{b_1} = 5$ $\gamma = 120^\circ$ | $a_1=0.7$ $b_1=0.14$ |

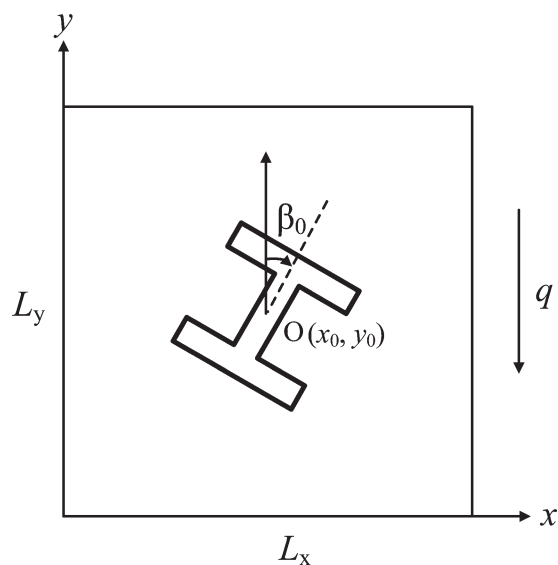


Figure 1. Schematic of a filler distributed in a cell model.

NUMERICAL WORK

Generation of Unit Cell Model

A two-dimensional elementary cell comprising of fillers in the base polymer material is considered. The cell is small and convenient for calculations, but large enough to represent a periodic section in the material. The fillers are assumed to be randomly distributed in the base materials with no aggregates. This is true when the filler content is below 20%. When the fillers are aggregated together, the mechanical strength of the composite materials will be seriously deteriorated.^{33,34} The fillers studied are around 1mm^2 each. The cell selected here is a $1 \times 1\text{cm}^2$ square, having a dozen of fillers, representing a periodic section in the composite material. The fillers may have different shapes and orientation angles on the two-dimensional surface. Table I lists 11 shapes of fillers considered in this study: spherical, square, equilateral triangular, rhombic, elliptical, rectangular, T shaped, I shaped, Y shaped, double Y shaped fillers and quad Y shaped. They are artificially designed, to evaluate the influences of filler shapes. They can be orient freely on the two dimensional x - y plane (Figure 1). In the table, their orientation angles are defined as 0° when the fillers' main axes (the vertical axes) overlap with the heat flux direction q .

Figure 1 demonstrates a filler distributed randomly in a unit cell. Its position and orientation angle can be specified by its coordinates (x_0, y_0) at the filler center and the orientation angle (β_0) between its main axis and the heat flux direction y .

In this research, a computer program is developed to automatically generate the positions and orientation angles of fillers distributed randomly in the cell.^{35,36} At first, the positions for the filler centers are determined. Let coordinates (x_0, y_0) represent the positions of filler centers. Let L_x and L_y denote the length and height of the unit cell respectively, as shown in Figure 1. Then a random number r_x ($0 < r_x < 1$) is generated by the computer. The coordinate x_0 is selected as the product of r_x and L_x . In a similar way coordinate y_0 is obtained. At last, the orientation angles of the fillers are assigned. The orientation angle β_0 , defined

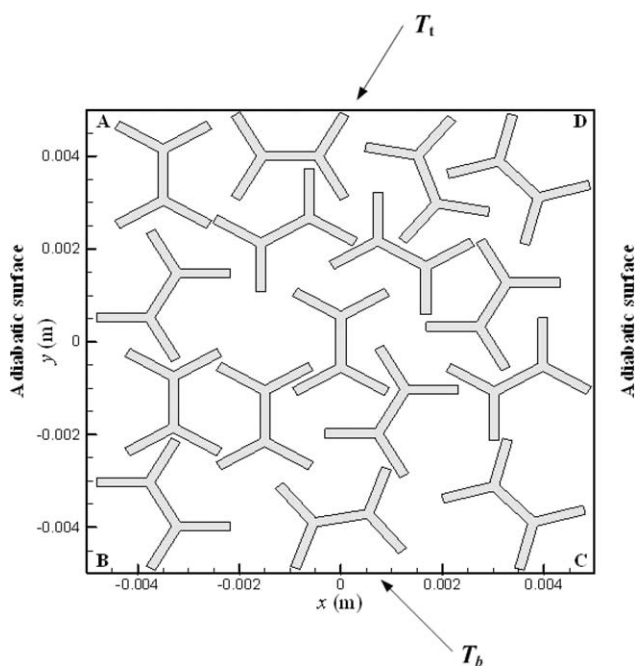


Figure 2. Two-dimensional cell model comprising of double Y shaped fillers and the base material, $V_f = 0.16$.

as the angle between the filler's main axis and the heat flux direction, is decided as the product of 2π and a random number from 0 to 1. In the process of filler generation, if a new filler is found to overlap with any other old fillers or boundaries, it is cancelled and a new one is generated. The filler generation process ends when a desired filler content is reached. The average orientation angles to the x - and y -axis are basically identical and the difference is controlled to within 2%.^{35,36} Figure 2 shows a generated fillers distribution. The filler type is double Y and the filler content is 16%. As seen, the fillers distribution in the cell is quite randomly. This is in agreement with practical composite materials. The fillers are mixed with the base material completely, so they are quite randomly distributed.

In order to build a model of composite of random structure, a minimum number of fillers must be included in the model. If the number of fillers is too small, results of each generation may be somewhat different. Consequently, the size of model must be chosen to be large enough to contain the minimum number of fillers, as long as computer capacity permits.

Figure 3 presents the effects of computational model sizes on the relative thermal conductivity at different volume fractions. As seen, when the model size becomes larger than 0.3cm^2 , the thermal conductivity is stable and the fluctuations from randomness is lower than 3%, regardless of the filler content. The differences of thermal conductivity in x - and y - directions are within 2%. In this study, the cell selected here is a $1 \times 1\text{cm}^2$ square. It is large enough for this two-dimensional thermal conductivity calculation.

Heat Conduction Equations

For the two-dimensional cell generated in Figure 2, heat conduction in base materials is satisfied by

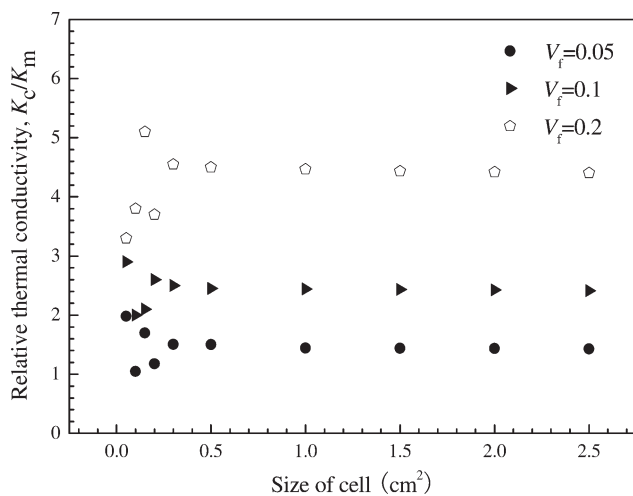


Figure 3. Effects of model sizes on the relative thermal conductivity of composite, $K_m = 0.36 \text{ Wm}^{-1} \text{ K}^{-1}$, $K_f = 50.2 \text{ Wm}^{-1} \text{ K}^{-1}$.

$$\frac{\partial^2 T_m}{\partial x^2} + \frac{\partial^2 T_m}{\partial y^2} = 0 \quad (1)$$

where T is temperature and x, y are coordinates, subscript “ m ” means base polymer materials.

Heat conduction in the fillers

$$\frac{\partial^2 T_f}{\partial x^2} + \frac{\partial^2 T_f}{\partial y^2} = 0 \quad (2)$$

Uniform and constant temperature is assumed at the cell top and bottom surfaces. At the top surface of the cell, AD, the boundary condition is

$$T_m|_{\text{top}} = T_t \quad (3)$$

At the bottom surface of the cell, BC, the boundary is

$$T_m|_{\text{bottom}} = T_b \quad (4)$$

In this numerical work, T_t is set to 310 K; and T_b is set to 290 K. In this problem, the average heat flow through the cell should be calculated by the heat conduction equations and the boundary conditions.

The other two boundary conditions, AB, DC

$$\frac{\partial T}{\partial n}|_{\Gamma} = 0 \quad (5)$$

they are assumed adiabatic.

Table II. Time Consumed in Calculation with Different Mesh Numbers with 16% Double Y Fillers

| Mesh number | Meshing time (s) | Calculation time (s) | Relative thermal conductivity |
|-------------|------------------|----------------------|-------------------------------|
| 100×100 | 5 | 30 | 3.43 |
| 150×150 | 15 | 60 | 3.43 |
| 200×200 | 25 | 100 | 3.42 |
| 250×250 | 40 | 150 | 3.42 |

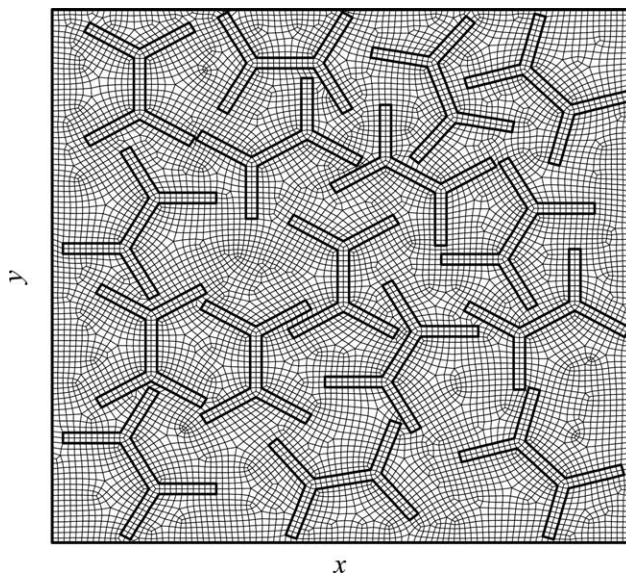


Figure 4. The mesh structure of the cell: double Y-shaped fillers with filler content 16%.

Heat Conduction Coupling

At the boundaries between the base materials and the fillers, the temperatures in the base materials are equaled to the fillers. They are expressed as

$$T_{m, \text{interface}} = T_{f, \text{interface}} \quad (6)$$

where subscript “interface” means contact surfaces between the base materials and the fillers.

When the temperature fields in the cell are calculated, the effective thermal conductivity in y direction for the cell is estimated by

$$K_c = \frac{qL_y}{T_t - T_b} \quad (7)$$

where q is the area mean heat flux at a cross section normal to the y direction. T_t and T_b are the uniform and constant temperature at the top and bottom surfaces. Dimensions L_x (along the x axis) and L_y (along the y axis) are the cell length and height.

Calculation Scheme and Solution

Equations (1)–(7) for conjugated heat conduction in the base materials and fillers are solved by finite difference technique. The cell is discretized by finite volume method.

The discretized equations are solved by central difference scheme. The calculation methodology can be summarized as following:

1. Assume initial temperature values for both the filler and the base materials.
2. Solve Eq.(1), get the temperature fields in the base materials, using the temperature values for fillers at interface as the boundary values for the base materials.
3. Solve Eq.(2), get the temperature fields in the fillers, taking the just calculated base material temperatures at interface as the boundary values.

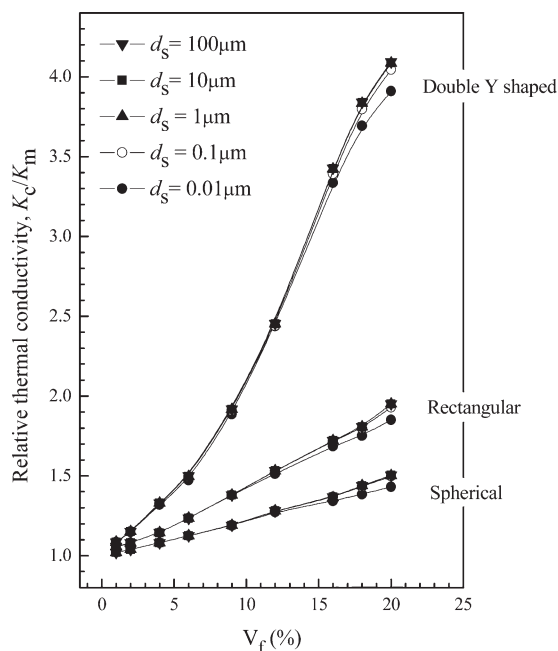


Figure 5. Effects of thermal interfacial resistance (R_b) on the thermal conductivity of 2Y, rectangular and spherical fillers filled composites with different filler sizes at 300K ($K_f = 50.2 \text{ Wm}^{-1} \text{ K}^{-1}$, $K_m = 0.36 \text{ Wm}^{-1} \text{ K}^{-1}$).

- Return to step (2) until all the old values and new values for both the base materials and the fillers are converged. In this way, the heat conduction equations are satisfied.

To assure the accuracy of the results calculated, a grid independence test is conducted. For a sample with double Y-shaped fillers. The size of the cell is 0.01 m. The volumetric content of filler is 16%. The calculated relative thermal conductivity and the time consumed in meshing and calculation are concluded in Table II. The time required to perform the analysis is greatly increased as the mesh refinement increases. However, no obvious change is observed for the results. Grid independence test is done and numerical uncertainty is within 0.3%. It indicates that meshes with 100×100 grids are adequate for this problem, which is less than 0.3% difference compared with 200×200 grids. The computational mesh is shown in Figure 4. A validated commercial software-FLUENT is used in the analysis to calculate temperature fields. When the average heat flux on the y direction are known, the effective thermal conductivity is calculated by eq. (7).

Thermal Interfacial Resistance

Contact resistance is due to the roughness of the surfaces in contact, which makes the effective area of contact less than the area of surfaces. The fillers can be completely wetted by the liquid polymer and they can be in perfect contact with base materials. Therefore, the contact resistance between the polymer and the fillers can be neglected.³⁷ Further, the filler generation program ensures that no fillers are in direct contact. So filler-to-filler contact resistance is not considered.

However, the fillers and the base polymer are different materials with different properties like densities, Debye temperatures, frequencies and speeds of sound. These differences result in

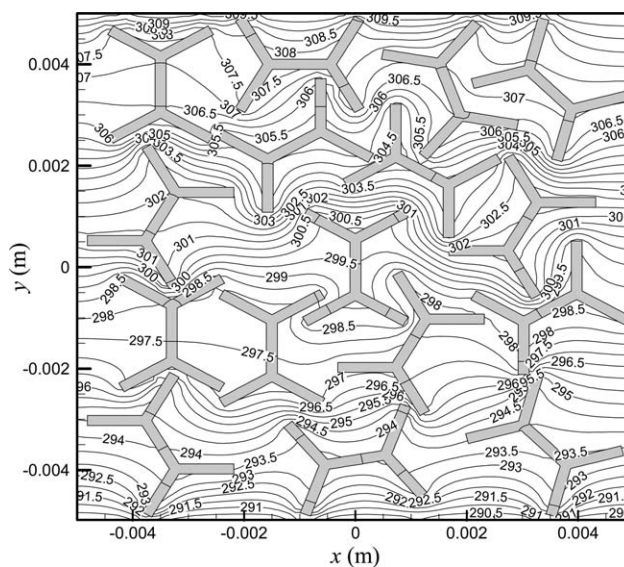


Figure 6. Contours of temperature (K) in the sample cell with 16% double Y shaped fillers.

resistances to the flow of phonons at the boundaries between them. It is called thermal interfacial resistance (R_b).³⁸ R_b was first measured by Kapitza in 1941 when he experimented on metal-liquid helium planar interfaces. That is the reason why the thermal resistance between the metal-liquid helium interfaces is known as the Kapitza resistance.³⁹

For the composites where high conductive particles are dispersed in a continuous matrix, the Kapitza radius α_K is often used, which is defined as

$$\alpha_K = R_b K_m \quad (8)$$

where K_m is the thermal conductivity of the base polymer, R_b is the thermal interfacial resistance. The Kapitza radius is in principle the critical particle size. If the filler particle radius is smaller than the α_K , the thermal conductivity of composites will be lower than that of the polymer material. It would decrease as the filler fraction increases. The interfacial thermal barrier acts as a thermal insulating coating. The smaller the filler particle is, the thicker the coating is.⁴⁰ The critical particle size for steel fillers in a wax matrix at room temperature is 3 nm.³⁷ The interfacial thermal conductivity can be specified by considering the thickness of the interface as a very small constant and thus⁴¹

$$K_s = \frac{K_m \delta}{\alpha_K} \quad (9)$$

where K_s is the thermal conductivity of the interface layer, δ is the thickness of the interface layer surrounding the filler. In this study, K_m is thermal conductivity of polymer (around $0.36 \text{ Wm}^{-1} \text{ K}^{-1}$), α_K equals critical particle size (3 nm). Assuming the interfacial layer is formed by air ($0.024 \text{ Wm}^{-1} \text{ K}^{-1}$), the thickness (δ) can be estimated by eq. (9). The value of δ is $2 \times 10^{-10} \text{ m}$.

Adding the interfacial air layer to the interfaces between the steel fillers and polymer matrix permits the calculation of the effective conductivity of the composites. The effects of interfacial thermal resistance are thus considered.⁴²

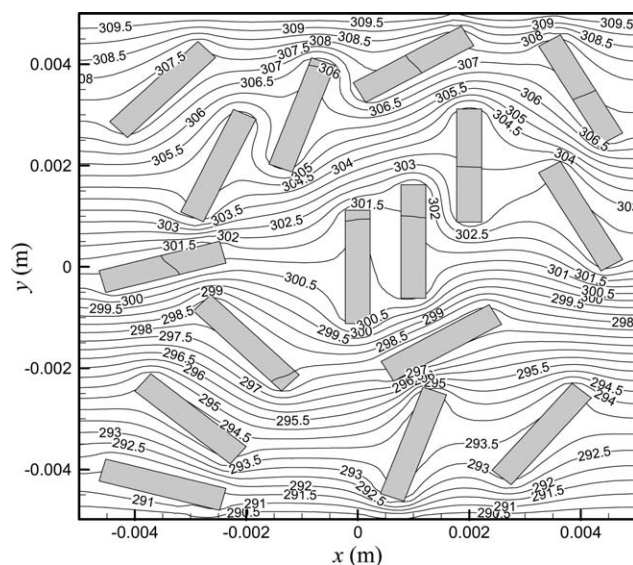


Figure 7. Contours of temperature (K) in the cell with 16% rectangular fillers.

Figure 5 shows the effects of interfacial layers on the thermal conductivity of filled composites. The studied filler shapes include: double Y-shaped, rectangular, and spherical. Filler sizes (d_s) are defined as the diameter of the circular filler circumference. Paraffin is used to simulate the polymer. Five different filler sizes are considered in this study. The graphs clearly indicate that R_b adversely affects the thermal conductivity of composites. The effect of interfacial thermal resistance is the same for different shapes fillers. It has larger effects at small filler sizes and larger volume fractions. When the filler sizes are greater than $1 \mu\text{m}$, the effects of R_b are very inconspicuous. At room temperatures, their effects are very small. The particle sizes should be in the nanoscale ranges to have a significant effect.

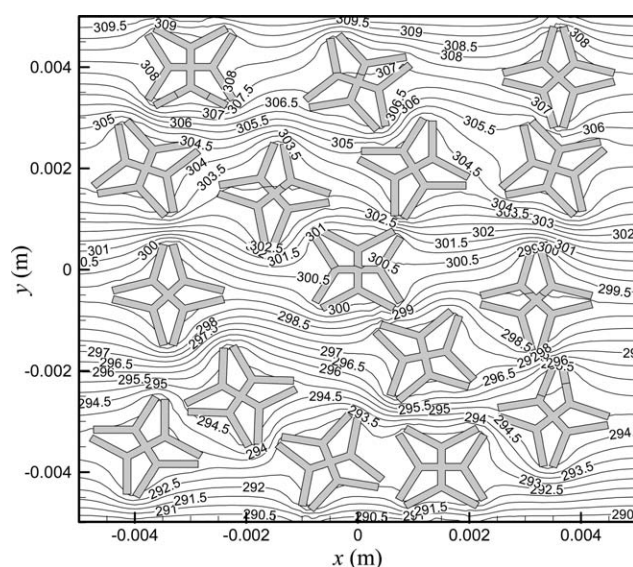


Figure 8. Contours of temperature (K) in the cell with 16% quad Y shaped fillers.

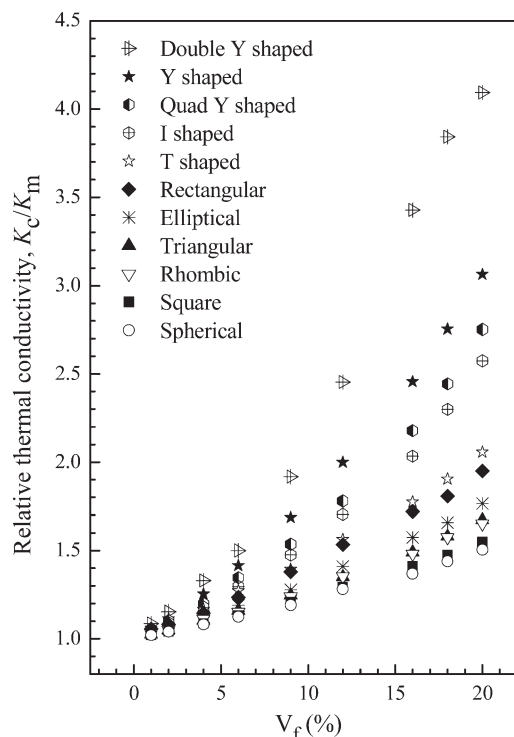


Figure 9. Relative thermal conductivity of composite materials with fillers of various shapes.

RESULTS AND DISCUSSION

Effects of Filler Shapes

To theoretically study the effects of filler shapes, temperature fields in the cell are calculated. An experiment will be done later to simulate the heat conduction in composite polymer materials. The composite material studied here is composed of paraffin wax and steel. Paraffin wax (melting point 60.2°C , conductivity $0.36 \text{ Wm}^{-1} \text{ K}^{-1}$) is used as the base material instead of polymers because it has a low melting point and it is easily processed in experiments. The filler material is steel (conductivity $50.2 \text{ Wm}^{-1} \text{ K}^{-1}$) because it is cheap and easily manufactured. Using the materials selected, the temperature fields are calculated. Still taking the cell with double Y fillers (Figure 2) as an example, temperature contours in the cell are plotted in Figure 6. The volumetric filler content is 16%. It can be seen that the effects of the fillers are great. The temperature fields in the base materials are deformed and shortcut by fillers. The fillers act as numerous bridges, transporting the heat fluxes through them. For each bridge, it absorbs heat at the upstream, and releases the heat at the downstream. The base material near the filler seldom takes part in heat transport, rather, it is shortcut. In this way, the heat transport is increased in the cell.

The orientation angle of 0° has the largest effects in increasing thermal conductivity. The angle of 90° has the worst effects. If all the filler are arranged orderly with a 0° orientation angle, thermal conductivity will be the highest. However a random distribution will comprise the fillers effects. The fillers distribute randomly in the base material. They have different orientation angles, resulting in different heat transporting distances, and

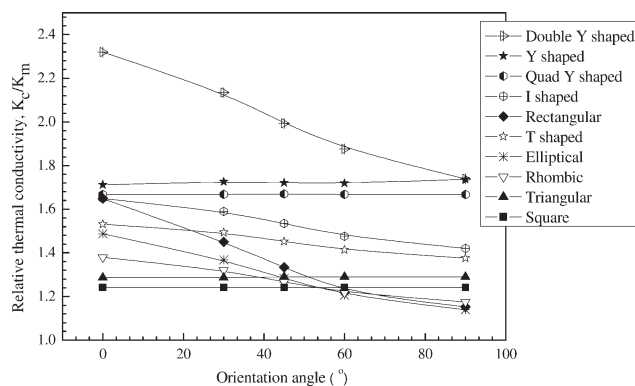


Figure 10. Relative thermal conductivity of composite materials in response to filler orientation angles, at a fixed volumetric filler content of 10%.

different contacting areas at upstream and downstream. The less the orientation angles are, the more efficient the fillers are in transporting heat. For good fillers, the contact areas both at the upstream and at the downstream should be larger enough to absorb heat from upstream and to release it to downstream, even when they are distributed randomly. Obviously the double Y fillers are such a choice. They have large contact areas and long heat conductance distances even when they are placed in the worst positions with a 90° orientation angle. In other words, they are quite robust in heat transport.

In contrast, the fillers of rectangular shapes are inferior. Figure 7 shows the temperature contours in a cell with fillers of rectangular shapes. The volumetric filler content is also 16%. As seen, the fillers are distributed randomly. When they are placed vertically (0° orientation angles), the heat transport distances are the largest. When they are placed horizontally, though upstream and downstream contact areas are larger, the heat transport distances are decreased drastically. As a result, they are less effective in enhancing heat conduction.

The fillers of quad Y-shaped are in the middle. Figure 8 shows the temperature contours in a cell with fillers of quad Y shaped. The volumetric filler content is also 16%. The filler is very like a sphere, but it is highly branched. The contact areas and heat conductance distances have no change with orientation angle. So, quad Y-shaped fillers is effective in enhancing heat conduction.

All the proposed fillers shapes listed in Table I are modeled. The base material is paraffin, and the filler material is steel, as already indicated. Heat conduction and temperature fields in the composite materials are modeled. The effective thermal conductivity of these composites is then calculated and compared for different filler shapes.

Figure 9 shows the relative thermal conductivity (K_c/K_m) for various filler shapes at different filler contents. As seen, the thermal conductivity increases with filler content, regardless of the filler shapes. However, the steps of increase are different. The double Y filler has the highest rate of increase, while the spherical filler has the least. The order for thermal conductivity increasing is: double Y > Y > quad Y > I > T > rectangular >

Table III. Constant in the Correlations for Various Filler Shapes

| Shape of filler | B_0 | B_1 | B_2 |
|-----------------|-------|-------|-------|
| Double Y shaped | 0.548 | 7.563 | 0.009 |
| Y shaped | 0.725 | 5.842 | 0.006 |
| Quad Y shaped | 0.802 | 4.972 | 0.004 |
| I shaped | 0.814 | 4.449 | 0.003 |
| T shaped | 0.881 | 3.664 | 0.002 |
| Rectangular | 0.892 | 3.643 | 0.002 |
| Elliptical | 0.897 | 3.878 | 0.002 |
| Rhombic | 0.941 | 2.647 | 0.001 |
| Triangular | 0.937 | 2.646 | 0.001 |
| Square | 0.953 | 2.294 | 0.001 |
| Spherical | 0.960 | 2.139 | 0.001 |

elliptical > rhombic \approx triangular > square \approx spherical. At the same filler contents of 0.2, the thermal conductivity with double Y fillers is 1.8 time higher than that with spherical fillers. The difference is due to the filler shapes, since they have substantial effects on the temperature fields and consequently the thermal conductivity. The Y and double Y shaped fillers are like trees. From this result, tree-like fillers are better than other regular shapes. In future industrial application, tree-like fillers should be searched.⁴³ From above analysis, it can be concluded that the best fillers are those that have long heat conductance distances and larger contact areas even when they are distributed randomly.

The effects of orientation angles of fillers can be analyzed theoretically by the numerical model. All fillers are distributed in the cell with same orientation angles. Figure 10 shows the relative thermal conductivity of composite materials in response to filler orientation angles, at a fixed filler content of 10%. When the angle is 0° , all fillers are arranged as those in Table I. Their main axes are the same as the input heat flux direction. In these cases, they have the largest contribution for thermal conductivity improvement. On the contrary, when the fillers are orientated to 90° , all the fillers have the minimum contribution for heat conduction augmentation.

The effects of orientation angles are complex for different fillers. The rectangular and double Y shaped fillers are the most sensitive. The effective thermal conductivity decreases drastically with increasing orientation angles. However the final conductivity of double Y shaped is still the largest. Some fillers are insensitive to orientation angles, like quad Y shaped, Y shaped, triangular, square. The I shaped and T shaped fillers are in the middle. They decrease somewhat with orientation angles, however the final conductivity is still acceptable. This behavior has no relation with filler content.

Correlations

Correlations are convenient for evaluation of thermal conductivity of composite materials, from engineering points of view. Previous correlations in literature^{11–24} didn't consider the interactions between the filler shapes and the base materials. Based on the data regression of numerical results, following

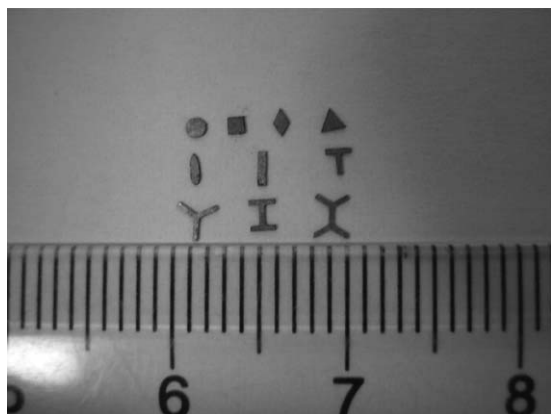


Figure 11. Photograph of the steel fillers made. The minimum reading on the ruler is 1 mm. [Color figure can be viewed in the online issue, which is available at wileyonlinelibrary.com.]

correlations are proposed for the estimation of effective thermal conductivity of composite materials with fillers of different shapes:

$$K_c = B_0 K_m + B_1 K_m V_f + B_2 K_f \quad (10)$$

Thermal conductivity of the composite materials is governed by factors like K_m , K_f , and V_f . The coefficients in the equations show the magnitude of their effects. The larger the coefficients are, the greater the contributions of these factors are. The regression $R^2 = 0.997$. The constants in the correlations for different filler shapes are listed in Table III. The applicable filler content ranges are $0.01 \leq V_f \leq 0.20$, and K_f/K_m less than 100. When K_f/K_m exceeds 100, K_f must be replaced by $100K_m$. The reason is that when the filler thermal conductivity is 100 times greater than that of the base material, there is no significant further improvement in the thermal conductivity of the composite materials.⁴⁴ In other words, there is little use by solely increasing the thermal conductivity of fillers, if the fillers conductivity has already been 100 times higher than the base materials. Further, for most filler filled composites, the filler content is greater than 1% to have real improvements in conductivity. At higher filler contents (>20%), filler aggregates would usually happen, and the correlations are no longer valid. Under such high content, composite materials

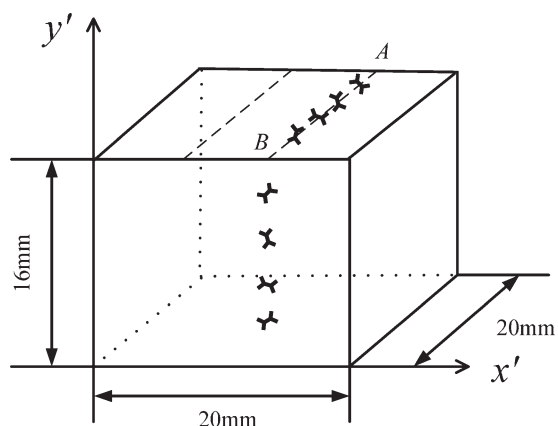


Figure 12. Dimensions of the composite wax plate made for experiment.

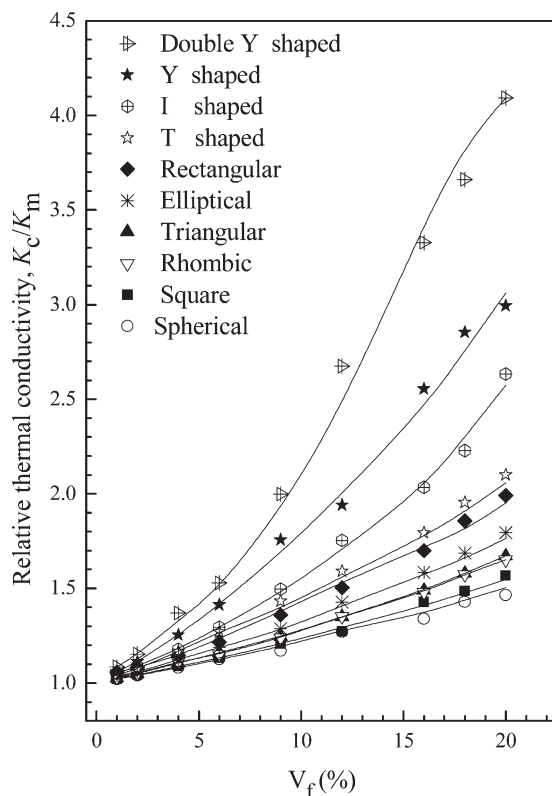


Figure 13. Comparisons of experimental and numerical thermal conductivity values for composites with various shaped fillers. Solid lines represent the data obtained by the correlations. The discrete points are the measured value.

will become brisk and they will lose mechanical durability and use.

EXPERIMENTAL STUDY

As mentioned, an experiment is done to simulate the composite materials. To validate the methodology, steel fillers of 10 different shapes are made. The shapes and their parameters have been shown in Table I. The dimensions in Table I are in mm. They are fixed values. These fillers have different shapes, but their areas are equal (around 1 mm^2). The thickness of the fillers is 0.2 mm. To make the casting process of composite materials easy, paraffin wax is used as the base material instead of plastics because of its low melting point. A steel foil of 0.2 mm thick is machine-cut into small pieces and then machined into the required shapes. The photographs of the machined fillers are shown in Figure 11. Steel is used as the filler material to save expenses.

After the fillers are prepared, the wax is placed in a metal box and melted under high temperature (70°C) in a water bath. The dimensions of the wax plate to be formed are schematically shown in Figure 12, 16 mm in thickness, 20 mm in depth and length. Then the fabricated fillers are placed along the x' - y' plane (perpendicularly to depth) into the melted paraffin wax at positions redetermined along the dashed lines (such as AB) in Figure 12. The randomness is ensured by a program to generate the random angles and positions. The number of fillers

are calculated and controlled according to the desired filler contents. Ten fillers are stacked along each dashed line to fill the wax depth (perpendicular to $x'-y'$), therefore the composite material can be assumed two dimensional in x' and y' . The melted wax is very viscous and it is almost half-solidified, so the fillers can stay there stably. The positions and the angles are controlled by a ruler system on the test table, with an accuracy of $\pm 0.1\text{mm}$. After the filling process completed, the wax is cooled down and solidified completely. Then the composite wax plate formed is removed from the metal box and its thermal conductivity is measured at 30°C by Hot Disk (DRX-2) equipment. The uncertainty for thermal conductivity measurement is 3%. To reduce this uncertainty, measurements are repeated 5 times for one sample. Meanwhile, three samples are made for each volume fraction and particle type. The effective thermal conductivity of three samples are stable and the differences are within 3%. The heat flux direction is y' .

Figure 13 shows the measured data for the composite materials made. Also shown are the data calculated by the correlation eq. (11), i.e., the numerical results predicted by the model. As can be seen, the trends of the tested thermal conductivity are same as the numerical results. The experimental values are in good agreement with the numerical results. The maximum deviation is less than 5%.

The fillers tested are relatively large for the easiness in making composite materials. They are in macro-scale. In future applications, the scale can be reduced, for instance to 10–100 micro meters, to mixed well with the base material and to ensure mechanical strength of the composite material. The method to make them in large scale should be searched. One possible solution may be chemical etching. This study just gives a fundamental research for future research directions.

CONCLUSIONS

The addition of highly conductive fillers in the polymer matrix is an effective way to increase thermal conductivity of the polymers. However, the effects of filler shapes on the thermal conductivity of composite materials, especially when the fillers are distributed randomly, were unknown before. The study here addresses this problem by investigating the effects of 11 artificially designed filler shapes. Following results can be concluded:

1. Best fillers should be tree-like. They should have long heat conduction distances and large contact areas even when they are placed unfavorably. From this respect, the double Y shaped fillers are the best, followed by Y shaped fillers. The spherical fillers are the worst. In future industrial applications, artificially designed filler shapes such as double Y, Y, I, quad Y shaped and T shaped should be used to replace the traditional filler shapes like particles, fibers and slice-like fillers.
2. A new correlation considering the filler shapes is proposed for estimation of effective thermal conductivity of composite materials where artificially designed fillers are distributed randomly in the base materials.
3. The simulation experiment with paraffin wax is successful in validating the methodology and the effects of filler shapes.

ACKNOWLEDGMENTS

The Project is supported by Natural Science Foundation of China, No. 51161160562. It is also supported by the 12th Five-years National Key Technology R&D Program (Grant No. 2012BAJ02B07).

NOMENCLATURE

| | |
|--------|---|
| a_1 | sectional length |
| a_K | Kapitza resistance |
| A_0 | specific contact area |
| A_F | cross-section area (m^2) |
| AB | left boundary of cell |
| AD | top boundary of cell |
| b_1 | sectional length |
| BC | bottom boundary of cell |
| c_p | specific heat ($\text{kJkg}^{-1}\text{K}^{-1}$) |
| c_1 | sectional length |
| d_1 | sectional length |
| d_c | critical diameter (m) |
| d_s | size of filler |
| DC | right boundary of cell |
| K | thermal conductivity ($\text{Wm}^{-1}\text{K}^{-1}$) |
| l_0 | thickness (m) |
| L_x | length along the x axis |
| L_y | height along the y axis |
| n | normal direction |
| P_e | perimeter of filler (m) |
| q | heat flux (Wm^{-2}) |
| r | radius of sphere |
| R_b | thermal interfacial resistance (Km^2/W) |
| V | volumetric fraction |
| x, y | coordinates (m) |
| x_0 | coordinate of filler center (m) |
| y_0 | coordinate of filler center (m) |
| x' | coordinate in width (m) |
| y' | coordinate in height (m) |

Greek letters

| | |
|-----------|--|
| α | apex angle for triangle ($^\circ$) |
| β | apex angle for rhombus ($^\circ$) |
| β_0 | orientation angle ($^\circ$) |
| γ | apex angle for Y and double Y ($^\circ$) |
| δ | thickness of interface layer |
| ρ | density (kg/m^3) |

Subscripts

| | |
|-----|----------------|
| c | composite |
| f | filler |
| m | polymer matrix |
| t | top surface |
| b | bottom surface |

REFERENCES

1. Joen, C. T.; Park, Y.; Wang, Q. *Int. J. Refrig.* **2009**, *32*, 763.

2. Wang, Q.; Han, X. H.; Sommmers, A. *Int. J. Refrig.* **2012**, *35*, 7.
3. Liu, X. H.; Jiang, Y. *Energy Convers. Manage.* **2008**, *49*, 1357.
4. Mahmud, K.; Mahmood, G. I.; Simonson C. J. *Energy Buildings.* **2010**, *42*, 1139.
5. Vali, A.; Simonson, C. J.; Besant, R. W. *Int. J. Heat Mass Transfer.* **2009**, *52*, 5827.
6. Sphaier, L. A.; Worek, W. M. *Int. J. Heat Mass Transfer.* **2009**, *52*, 2265.
7. Weidenfeller, B.; Hofer, M.; Schilling, F. R. *Compos. Part A.* **2004**, *35*, 423.
8. Yaggee, F. L.; Gilbert, E. R.; Styles J. W. J. *Less Common Metals.* **1969**, *19*, 39.
9. Zhang, L. Z.; Wang, X. J.; Pei, L. X. *Int. J. Heat Mass Transfer.* **2012**, *55*, 7287.
10. Han, Z. D.; Fina, A. *Prog. Polym. Sci.* **2011**, *36*, 914.
11. Sofian, N. M.; Rusu, M. J. *Thermoplast. Compos.* **2001**, *14*, 20.
12. Yu, A.; Ramesh, P.; Sun, X. B. *Adv. Mater.* **2008**, *20*, 4740.
13. Bigg, D. M. *Polym. Compos.* **1986**, *7*, 125.
14. Lewis, T.; Nielsen, L. J. *Appl. Polym. Sci.* **1970**, *14*, 1449.
15. Nozad, I.; Garbonell, R. G.; Whitaker, S. *Chem. Eng. Sci.* **1985**, *40*, 843.
16. Whitaker, S. *Springer* **1998**, *1*, 425.
17. Nielsen, L. *Ind. Eng. Chem. Fund.* **1974**, *13*, 17.
18. Baschirow, A. B.; Manukian, A. M. *Mech. Eng.* **1974**, *3*, 564.
19. Bruggeman, D. A. *Ann. Phys.* **1953**, *24*, 636.
20. Agari, Y.; Uno, T. *J. Appl. Polym. Sci.* **1986**, *32*, 5705.
21. Agari, Y.; Ueda, A.; Nagai, S. *J. Appl. Polym. Sci.* **1991**, *43*, 1117.
22. Agari, Y.; Ueda, A.; Nagai, S. *J. Appl. Polym. Sci.* **1994**, *42*, 1665.
23. Tavman, I. H.; Akinici, H. *Int. Commun. Heat Mass.* **2000**, *27*, 253.
24. Halpin, J. C. J. *Compos. Mater.* **1969**, *3*, 732.
25. Sanada, K.; Tada, Y.; Shindo, Y. *Compos. Part A.* **2009**, *40*, 724.
26. Yang, S. Y.; Lin, W. N.; Huang, Y. L. *Carbon* **2011**, *49*, 793.
27. Fricke, H. *Phys. Rev.* **1924**, *24*, 575.
28. Nan, C. W.; Birringer, R.; Clarke, D. R. *J. Appl. Phys.* **1997**, *81*, 6692.
29. Duan, H. L.; Karihaloo, B. L. *Phys. Rev. B.* **2007**, *75*, 642.
30. Xie, H. Q.; Wang, J. C.; Xi, T. G. *J. Mater. Sci. Lett.* **2002**, *21*, 193.
31. Yang, B.; Han, Z. H. *Appl. Phys. Lett.* **2006**, *89*, 311.
32. Pan, Y.; Weng, G. J.; Meguid, S. A. *J. Appl. Phys.* **2011**, *110*, 3715.
33. Casado, U.; Marcovich, N. E.; Aranguren, M. I. *Polym. Eng. Sci.* **2009**, *49*, 713.
34. Masuko, T. *Kobunshi Ronbunshu.* **2004**, *61*, 489.
35. Xu, Y. B.; Yagi, K. C. *Comput. Mater. Sci.* **2004**, *30*, 242.
36. Phelan, P. E.; Niemann, R. C. *J. Heat Transf.* **1998**, *120*, 971.
37. Devpura, A.; Phelan, P. E.; Prasher, R. S. *Microscale Thermophys. Eng.* **2001**, *5*, 177.
38. Zhang, Q.; Pi, Z. H.; Chen, M. X. *J. Compos. Mater.* **2011**, *0*, 1.
39. Swartz, E. T.; Pohl, R. O. *Rev. Mod. Phys.* **1984**, *63*, 605.
40. Wang, J. J.; Yi, X. S. *Compos. Sci. Technol.* **2004**, *64*, 1623.
41. Nan, C. W.; Birringer, R.; Clarke, D. R. *J. Appl. Phys.* **1997**, *81*, 6692.
42. Zeng, J.; Fu, R. L.; Simeon, A. J. *Electron. Packaging.* **2009**, *131*, 041006 (1).
43. Bejan, A.; Lorente, S. *Int. J. Engng. Ed.* **2008**, *22*, 140.
44. Bigg, D. M. *Polym. Compos.* **1986**, *7*, 125.